Supporting Information

Degradation mechanism of LiCoO$_2$ at a high voltage in a model all-solid-state battery with highly stable solid/solid interfaces

Kotaro Ito,[1] Kazuhisa Tamura,[2] Keisuke shimizu[3], Norifumi L. Yamada,[4] Kenta Watanabe,[1] Kota Suzuki,[3] Ryoji Kanno,[3] and Masaaki Hirayama[1,3]*

[1]Department of Chemical Science and Engineering, School of Materials and Chemical Technology, Tokyo Institute of Technology, 4259 Nagatsuta-cho, Midori-ku, Yokohama 226-8501, Japan

[2]Materials Sciences Research Center, Japan Atomic Energy Agency, 1-1-1 Koto, Sayo, Hyogo 679-5148, Japan

[3]Research Center for All-Solid-State Battery, Institute of Innovative Research, Tokyo Institute of Technology, 4259 Nagatsuta-cho, Midori-ku, Yokohama 226-8501, Japan

[4]Institute of Materials Structure Science, High Energy Accelerator Research Organization, 203-1 Shirakata, Tokai, Ibaraki 319-1106, Japan

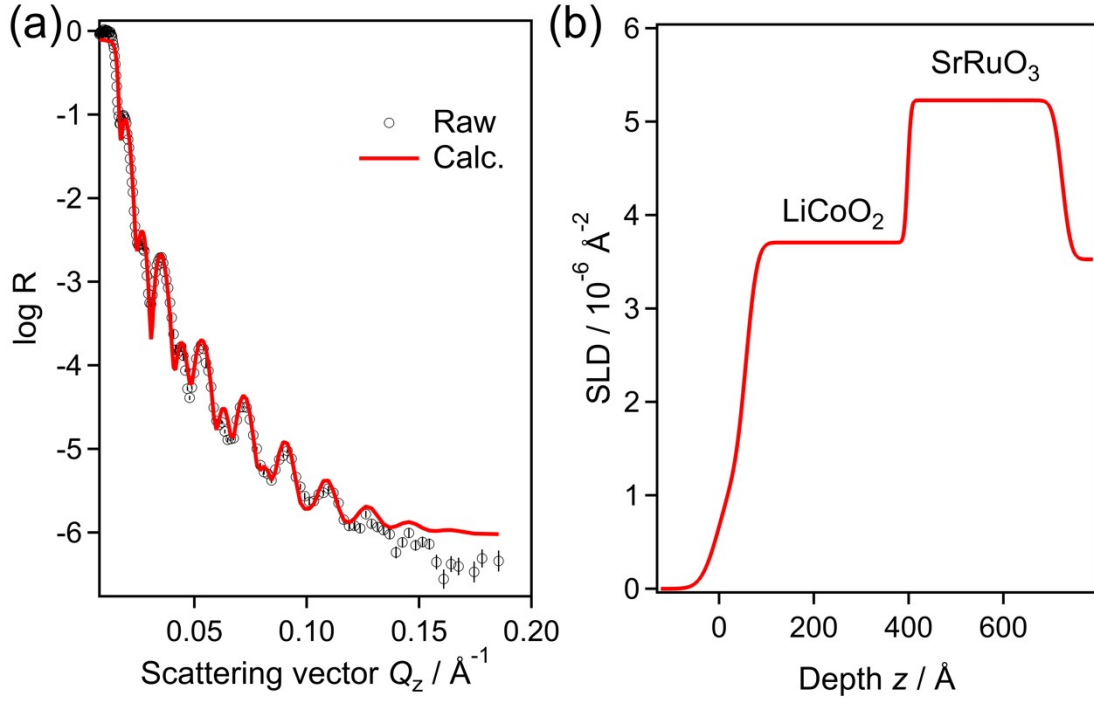Corresponding author e-mail: hirayama@mac.titech.ac.jp

Figure S1. Neutron reflectivity and simulated curve (a) and scattering length density profile (b) of the SrRuO$_3$/SrTiO$_3$(100) substrate prepared by RF magnetron sputtering.

The reflectivity spectrum was plotted as a function of the scattering vector, Q_z.

$$Q_z = 4\pi\sin\theta/\lambda \tag{1}$$

where θ is the glancing angle and λ is the wavelength of neutrons. A four-layer model (surface layer/LiCoO$_2$/SrRuO$_3$/SrTiO$_3$), including an impurity layer on the top surface, was used as the fitting model. The fits are in reasonable agreement with the experimental data ($\chi^2 = 1.8 \times 10^{-2}$).
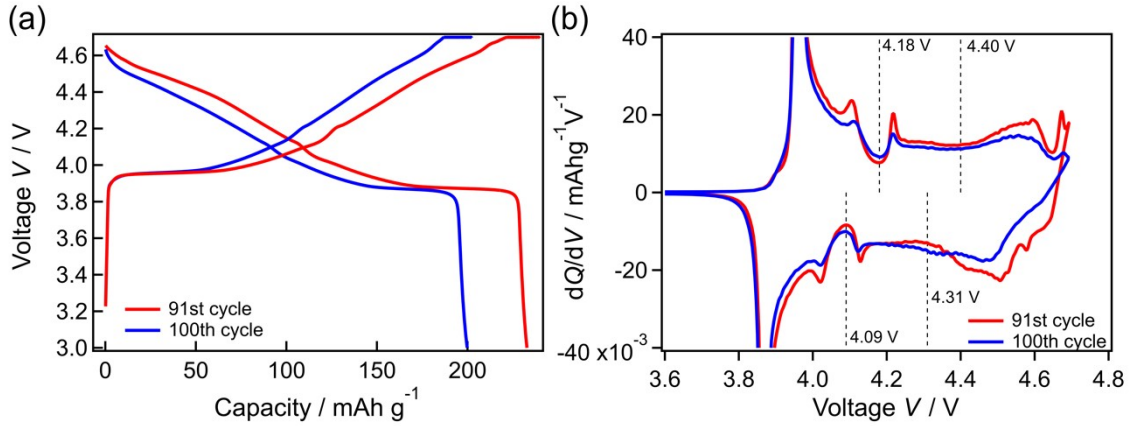
Figure S2. (a) Charge-discharge curves extracted only 91st and 100th cycle from Figure 4f. (b) Differential capacity (dQ/dV) plots obtained by (a).

Differential capacity plots were obtained from the charge–discharge curves recorded in the voltage range of 3.0 to 4.7 V (Figure 4f in the main manuscript). At 3.9 V, peaks that correspond to Li^+ (de)intercalation with the transition between two different hexagonal phases appeared. Small peaks were observed at 4.1 V in the charged state and 4.02 V in the discharged state. These peaks are due to hexagonal-to-monoclinic phase transition. Similarly, small peaks were observed at 4.22 V in the charged state and 4.13 V in the discharged state due to monoclinic-to-hexagonal phase transition. The peak positions of the above six peaks did not change with charge–discharge at 4.7 V. This result suggests that these phase transitions are not affected by the overvoltage caused by the appearance of the O1 structure. In the charged state, a peak at ~4.6 V and a rising peak at ~4.7 V were observed. These correspond to O3 → H1-3 and H1-3 → O1 phase transitions of $LiCoO_2$ (LCO), respectively. On the other hand, a single broad peak was observed in the discharged state. This result suggests that the phase transition from O1 to O3 progresses with difficulty. In this study, to compare the capacity decrease over different voltage ranges, three voltage ranges were defined: stage I is the voltage range up to the phase transition of the LCO material to monoclinic phase, including a major plateau at 3.9 V (charge: 3.0–4.18 V, discharge: 3.0–4.09 V), stage II is the voltage range for the phase transition of LCO to monoclinic and back to hexagonal (charge: 4.18–4.4 V, discharge: 4.09–4.31 V), stage III is the voltage range for phase transition from O3 to O1 (charge: 4–4.7 V, discharge: 4.31–4.7 V). The voltage for discharge was shifted by 0.09 V to account for the effect of overvoltage.
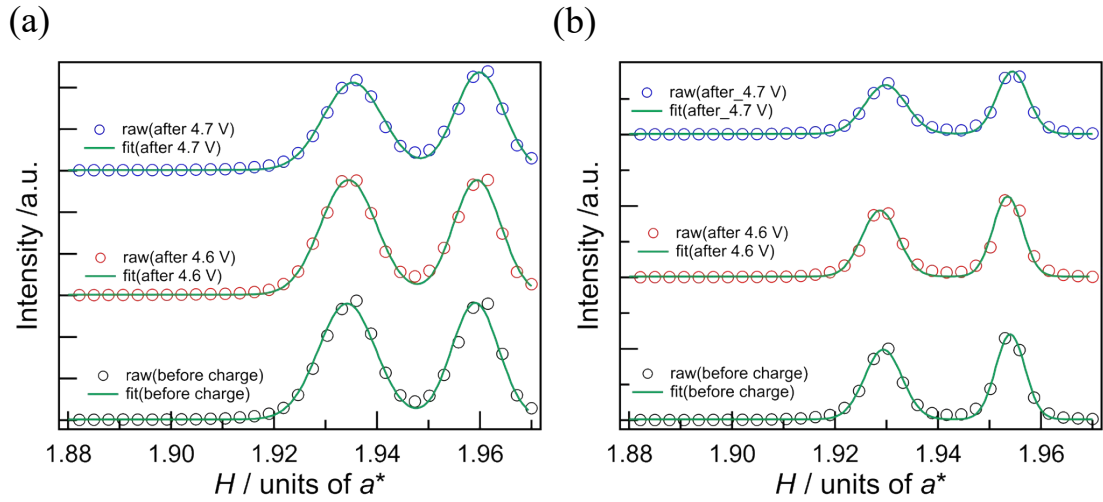
Figure S3. Synchrotron X-ray surface diffraction patterns (in-plane) of a thin-film battery (Li/Li$_3$PO$_4$/LiCoO$_2$/SrRuO$_3$/SrTiO$_3$) recorded via *HH*0 scan along the [110] direction of the SrTiO$_3$(100) substrate and the corresponding fits. Reflections of the regions near the bulk (a) and interface (b) were obtained by adjusting the incident angle of the synchrotron X-rays.

Figure S4. Synchrotron X-ray surface diffraction patterns (in-plane) of the thin-film battery (Li/Li$_3$PO$_4$/LiCoO$_2$/SrRuO$_3$/SrTiO$_3$) recorded via *H*00 scan along the [100] direction of the SrTiO$_3$(100) substrate and the corresponding fits. Reflections of the regions near the bulk (a) and interface (b) were obtained by adjusting the incident angle of the synchrotron X-rays.
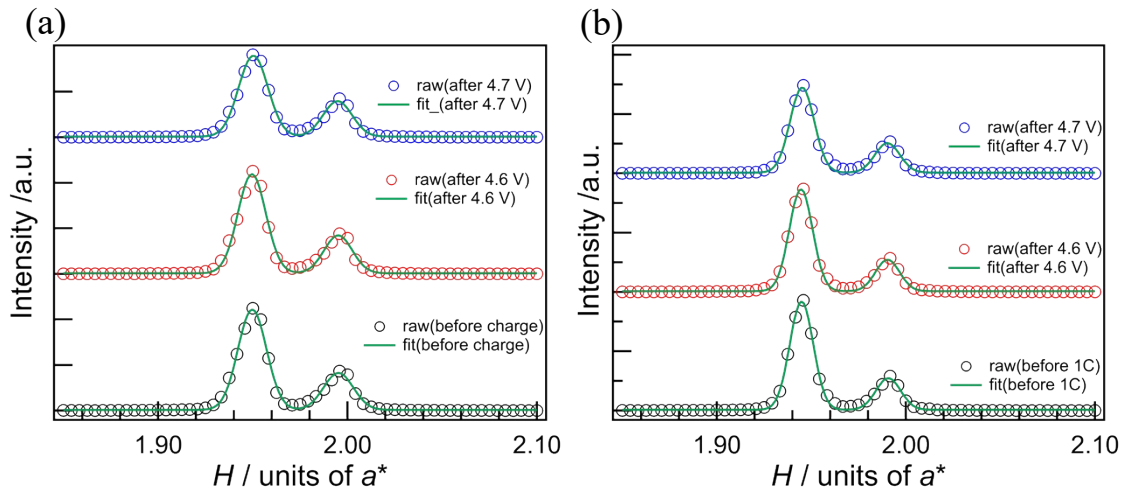
Table S1. Areas of the in-plane synchrotron X-ray surface diffraction peaks and peak area ratios calculated by least squares fitting for before and after 4.7 V charging.

Peak	Interface or bulk	(a) Peak area **before** charging	(b) Peak area of the discharged state **after** charging to **4.7 V**	Peak area ratio (b)/(a)
10-8	Interface	8.92×10^{-4}	6.91×10^{-4}	0.78
	Bulk	3.89×10^{-3}	3.05×10^{-3}	0.78
1−20	Interface	8.48×10^{-4}	6.66×10^{-4}	0.79
	Bulk	3.23×10^{-3}	2.78×10^{-3}	0.86
0−14	Interface	2.85×10^{-3}	2.31×10^{-3}	0.81
	Bulk	4.17×10^{-3}	3.46×10^{-3}	0.83